

Passion fruit-like microspheres of FeS₂ wrapped with carbon as excellent fast charging materials for supercapacitors

Xuexia Liu, Weizhen Deng, Limin Liu, Yinfeng Wang, Chunfang Huang, and Zhijun Wang*

College of Chemistry and Chemical Engineering, Jinggangshan University, Ji'an, Jiangxi 343009,
PR China

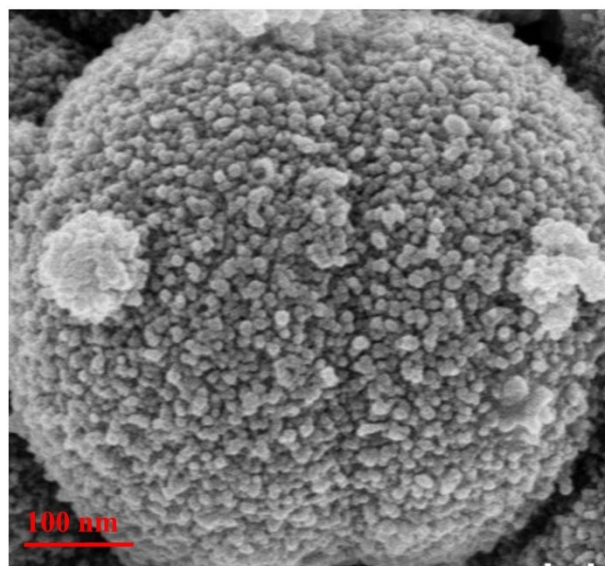


Fig. S1 SEM image of $\text{FeS}_2@\text{Carbon-3}$ microspheres.

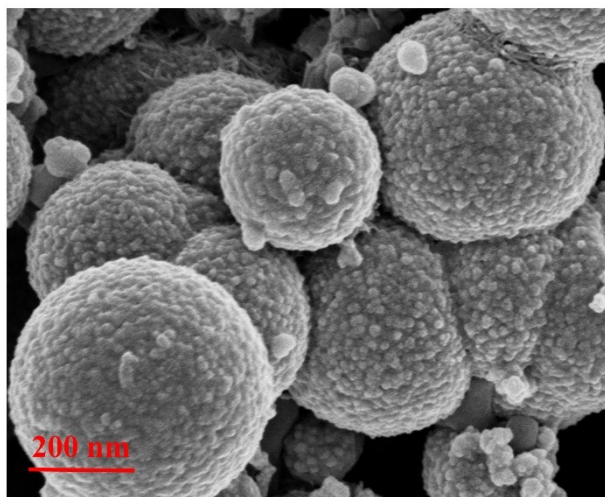


Fig. S2 SEM image of FeS₂@Carbon-0 microspheres.

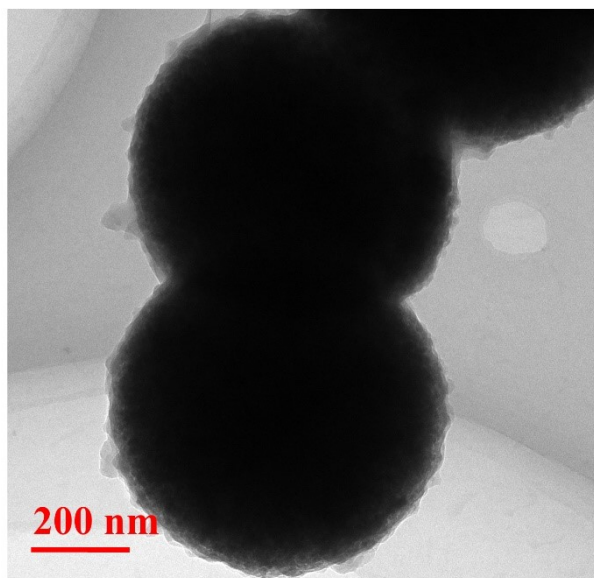


Fig. S3 TEM image of $\text{FeS}_2@\text{Carbon-0}$ microspheres.

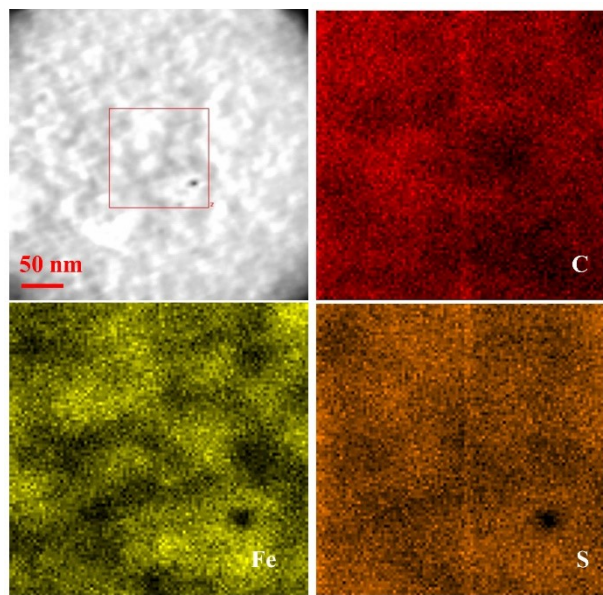


Fig. S4 Elemental mapping images of FeS₂@Carbon-3 microspheres.

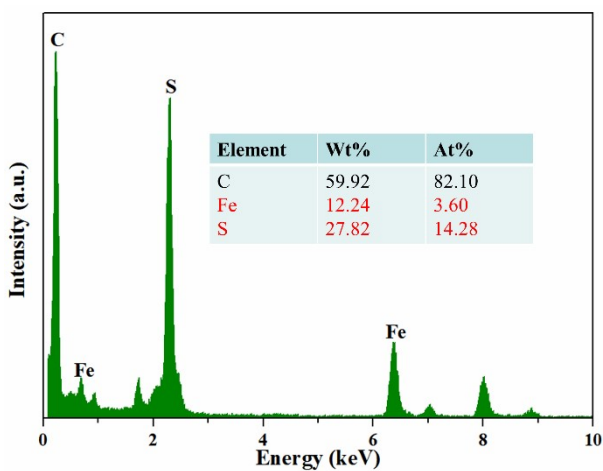


Fig. S5 EDX spectrum of FeS₂@Carbon-3 microspheres.

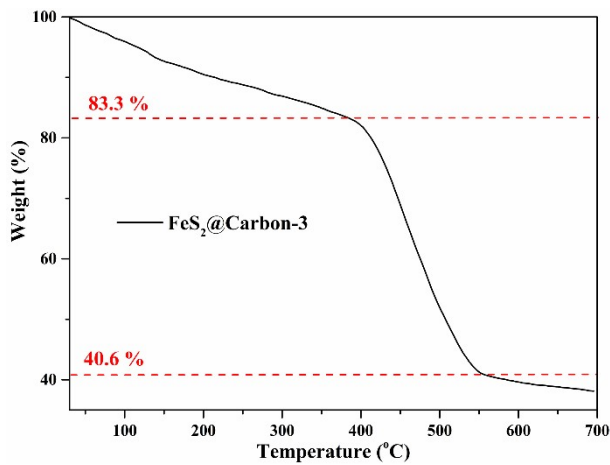


Fig. S6 TGA of $\text{FeS}_2@\text{Carbon-3}$ microspheres.

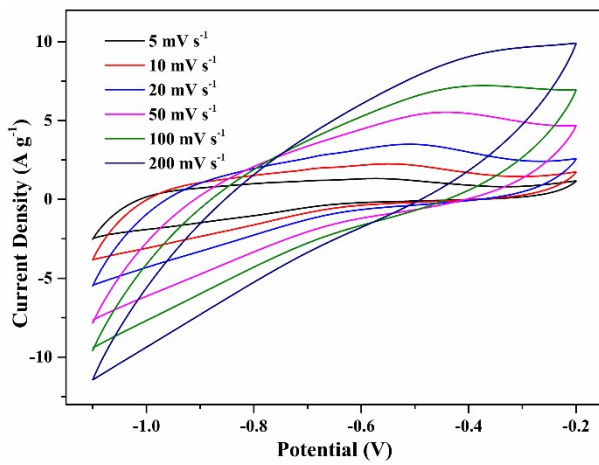


Fig. S7 CV curves of FeS₂ at different scan rates.

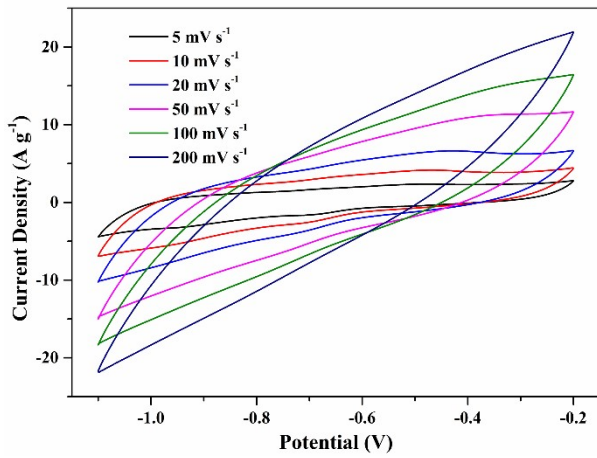


Fig. S8 CV curves of the $\text{FeS}_2@\text{Carbon-0}$ microspheres at different scan rates.

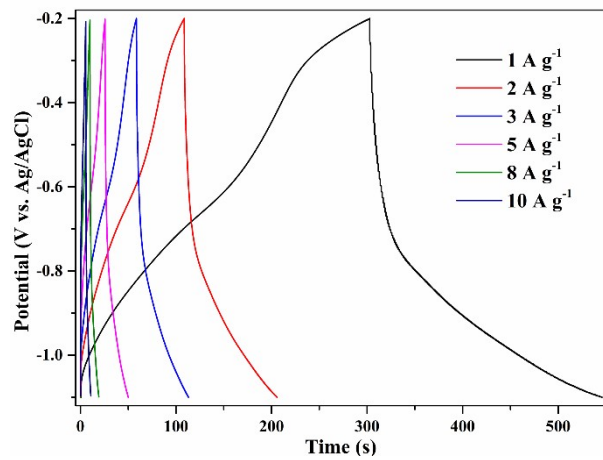


Fig. S9 Galvanostatic charge-discharge curves of FeS₂ microspheres at different current densities.

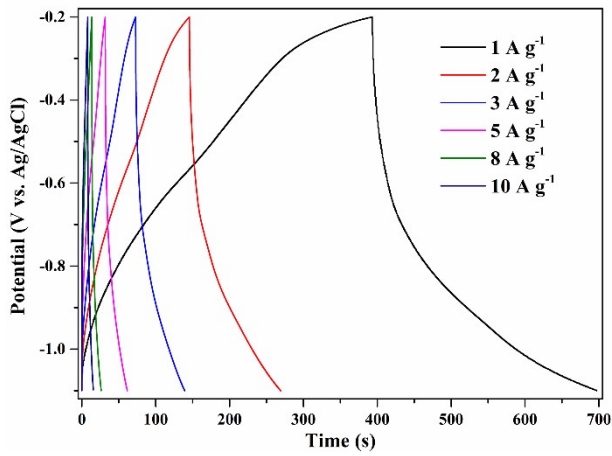


Fig. S10 Galvanostatic charge-discharge curves of FeS₂@Carbon-0 microspheres at different current densities.

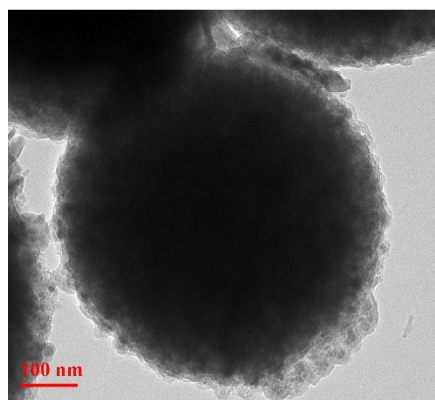


Fig. S11 TEM image of $\text{FeS}_2@\text{Carbon-3}$ microspheres after cycling test.

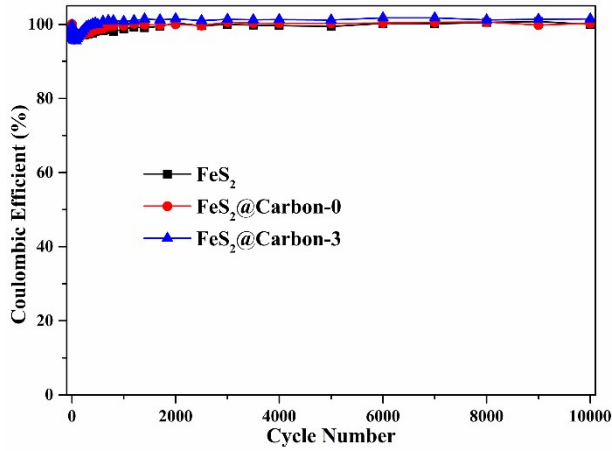


Fig. S12 The coulombic efficiency of FeS_2 , $\text{FeS}_2@\text{Carbon-0}$ and $\text{FeS}_2@\text{Carbon-3}$ microspheres at the current density of 5 A g^{-1} associated to the galvanostatic charge-discharge cycles.

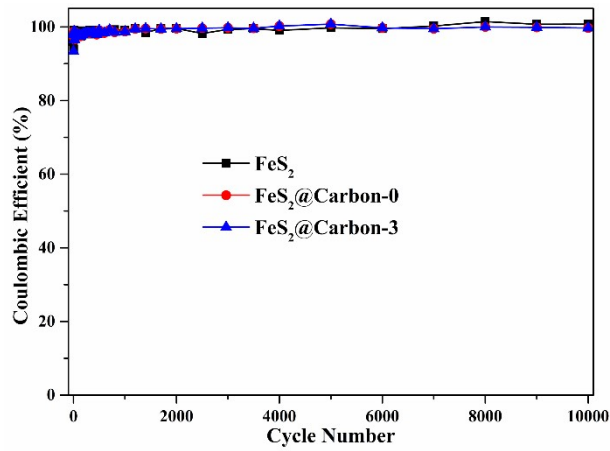


Fig. S13 The coulombic efficiency of FeS₂, FeS₂@Carbon-0 and FeS₂@Carbon-3 microspheres at the current density of 8 A g⁻¹ associated to the galvanostatic charge-discharge cycles.

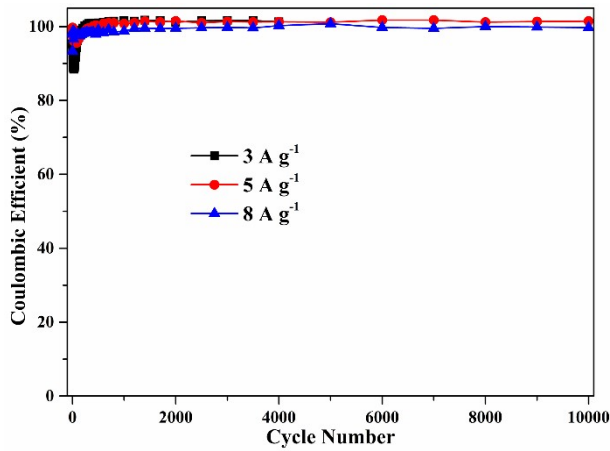


Fig. S14 The coulombic efficiency of FeS₂@Carbon-3 microspheres at different current densities of 3, 5 and 8 A g⁻¹ associated to the galvanostatic charge-discharge cycles.

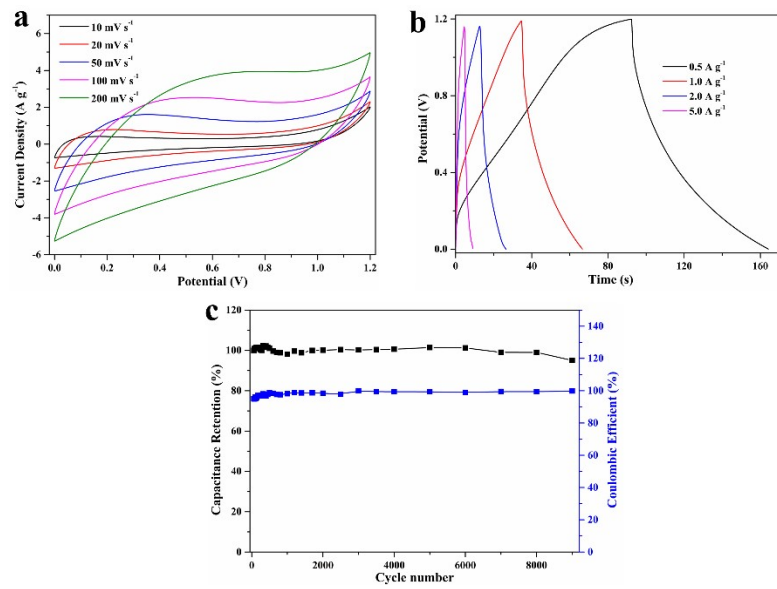


Fig. S15 (a) CV at different scan rates, (b) GCD curves at different current densities and (c) Long cycle performance of the HSC.

Table S1 The specific capacitance of FeS₂, FeS₂@Carbon-0 and FeS₂@Carbon-3 microspheres at different scan rates.

Scan rates (mV s ⁻¹)	Specific capacitance (F g ⁻¹)		
	FeS ₂	FeS ₂ @Carbon-0	FeS ₂ @Carbon-3
5	285.5	542.7	470.6
10	231.4	457.3	427.6
20	162.7	328.3	330.6
50	90.3	180.8	197.9
100	50.1	103.9	122.0
200	29.3	56.1	70.1

Table S2 The specific capacitance of FeS₂, FeS₂@Carbon-0 and FeS₂@Carbon-3 microspheres at different current densities.

Current density (A g ⁻¹)	Specific capacitance (F g ⁻¹)		
	FeS ₂	FeS ₂ @Carbon-0	FeS ₂ @Carbon-3
1	270.0	337.8	278.4
2	216.0	274.7	242.2
3	181.3	221.0	208.7
5	134.4	165.6	171.7
8	82.7	112.9	126.2
10	58.9	83.3	100.0

Table S3 Comparison the specific capacitance with some reported literature on FeS₂ composites for supercapacitors.

Materials	Electrolyte	Specific capacitance	Current density	Ref
FeS ₂ nano-alloys	30% KOH	406 F g ⁻¹	1 A g ⁻¹	1
FeS ₂ @Fe ₂ O ₃ hybrid	1M Li ₂ SO ₄	255 F g ⁻¹	1 A g ⁻¹	2
FeS ₂ nanobelts	1M Na ₂ SO ₄	317.9 F g ⁻¹	3 A g ⁻¹	3
FeS ₂ /GNS	2M KOH	793 C g ⁻¹	3 A g ⁻¹	4
FeS ₂ nanoellipsoids	2M KOH	515 C g ⁻¹	1 A g ⁻¹	5
FeS ₂ /graphene aerogel	6M KOH	268.7 F g ⁻¹	2 A g ⁻¹	6
FeS ₂ /Fe ₂ O ₃ @S-rGO	6M KOH	790 F g-1	2 A g ⁻¹	7
P-FeS ₂ /GNS	2M KOH	246 mAh g ⁻¹	3 A g ⁻¹	8
FeS ₂ nanotubes	3M KCl	320 F g ⁻¹	1.25 A g ⁻¹	9
FeS ₂ /MoS ₂ nanosheet	3M KOH	495 mF cm ⁻²	1 mA cm ⁻²	10
FeS ₂ /PVP composite	3M KOH	526.08 F g ⁻¹	1 A g ⁻¹	11
FeS ₂ /3DPC	1M KOH	304 F g ⁻¹	2 A g ⁻¹	12
Pyrite FeS ₂	3.5M KOH	206 F g ⁻¹	1 A g ⁻¹	13
Petal-like FeS ₂	6M KOH	321.3 F g-1	1 A g ⁻¹	15
FeS ₂ @Carbon-3	1M KOH	278.4 F g ⁻¹	1 A g ⁻¹	This work

Supporting References

- [1] V. Sridhar, H. Park, *J. Alloy. Compd.*, 2018, **732**, 799-805.
- [2] Y. Zhang, J. Q. Liu, Z. D. Lu, H. Xia, *Mater. Lett.*, 2016, **166**, 223-226.
- [3] J. Z. Chen, X. Y. Zhou, C. T. Mei, J. L. Xu, S. Zhou, C. P. Wong, *Electrochim. Acta*, 2016, **222**, 172-176.
- [4] Z. Q. Sun, H. M. Lin, F. Zhang, X. Yang, H. Jiang, Q. Wang, F. Y. Qu, *J. Mater. Chem. A*, 2018, **6**, 14956-14966.
- [5] Z. Q. Sun, X. Yang, H. M. Lin, F. Zhang, Q. Wang, F. Y. Qu, *Inorg. Chem. Front.*, 2019, **6**, 659-670.
- [6] L. Y. Pei, Y. Yang, H. Chu, J. F. Shen, M. X. Ye, *Ceram. Int.*, 2016, **42**, 5053-5061.
- [7] R. R. Bu, Y. Deng, Y. L. Wang, Y. Zhao, Q. Q. Shi, Q. Zhang, Z. Y. Xiao, Y. Y. Li, W. Sun, L. Wang, *ACS Appl. Energy Materials*, 2021, **4**, 11004-11013.
- [8] Z. Q. Sun, F. Z. Li, Z. Q. Ma, Q. Wang, F. Y. Qu, *J. Alloy. Compd.*, 2021, **854**, 157114.
- [9] Y. C. Chen, J. H. Shi, Y. K. Hsu, *Appl. Surf. Sci.*, 2020, **503**, 144304.
- [10] Y. R. Wang, Y. B. Xie, *J. Alloy. Compd.*, 2020, **824**, 153936.
- [11] I. K. Durga, S. S. Rao, R. M. N. Kalla, J. W. Ahn, H. J. Kim, *J. Energy Storage*, 2020, **18**, 101216.
- [12] Y. Y. Huang, S. Bao, Y. S. Yin, J. L. Lu, *Appl. Surf. Sci.*, 2021, **565**, 150538.
- [13] S. Venkateshalu, P. F. Kumar, P. Kollu, S. K. Jeong, A. N. Grace, *Electrochim. Acta.*, 2018, **290**, 378-389.
- [14] A. M. Zardkhoshouei, S. S. H. Davarani, A. A. Asgharinezhad, *Dalton Trans.*, 2019, **48**, 4274-4282.